Cell PRESS
Open ACCESS
Cell Reports
Article

A Design Principle for a Posttranslational Biochemical Oscillator

Craig C. Jolley,[1,7] Koji L. Ode,[3,7] and Hiroki R. Ueda[1,2,3,4,5,6,*]
[1]Laboratory for Systems Biology
[2]Functional Genomics Unit
RIKEN Center for Developmental Biology, 2-2-3 Minatojima-minamimachi, Chuo-ku, Kobe, Hyogo 650-0047, Japan
[3]Laboratory for Synthetic Biology, RIKEN Quantitative Biology Center, 2-2-3 Minatojima-minamimachi, Chuo-ku, Kobe, Hyogo 650-0047, Japan
[4]Department of Biological Sciences, Graduate School of Science, Osaka University, 1-1 Machikaneyama, Toyonaka, Osaka 560-0043, Japan
[5]Graduate School of Frontier Biosciences, Osaka University, 1-3 Yamadaoka, Suita, Osaka 565-0871 Japan
[6]Department of Mathematics, Graduate School of Science, Kyoto University, Kitashirakawa Oiwake-cho, Sakyo-ku, Kyoto, Kyoto 606-8502, Japan
[7]These authors contributed equally to this work.
*Correspondence: uedah-tky@umin.ac.jp
http://dx.doi.org/10.1016/j.celrep.2012.09.006

SUMMARY

Multisite phosphorylation plays an important role in biological oscillators such as the circadian clock. Its general role, however, has been elusive. In this theoretical study, we show that a simple substrate with two modification sites acted upon by two opposing enzymes (e.g., a kinase and a phosphatase) can show oscillations in its modification state. An unbiased computational analysis of this oscillator reveals two common characteristics: a unidirectional modification cycle and sequestering of an enzyme by a specific modification state. These two motifs cause a substrate to act as a coupled system in which a unidirectional cycle generates single-molecule oscillators, whereas sequestration synchronizes the population by limiting the available enzyme under conditions in which substrate is in excess. We also demonstrate the conditions under which the oscillation period is temperature compensated, an important feature of the circadian clock. This theoretical model will provide a framework for analyzing and synthesizing posttranslational oscillators.

INTRODUCTION

For a wide variety of organisms, biology runs on a schedule. The control of cellular and organismal processes by biochemical clocks has a number of potential advantages. The circadian clock system allows organisms to anticipate ecological changes that correlate with the day/night cycle, regulating both behavioral patterns and metabolic fluxes. The period of circadian rhythmicity is robust and fairly unaffected by the ambient temperature (Hastings and Sweeney, 1957; Pittendrigh, 1954).

Circadian clocks are thought to be driven by cell-autonomous transcriptional-translational oscillators (TTOs) (Dibner et al., 2010; Dunlap, 1999; Reppert and Weaver, 2002; Takahashi et al., 2008; Young and Kay, 2001). In mammalian clocks, the circadian transcriptional program is mediated by at least three clock-controlled DNA elements, known as morning-time (E-box/E′-box or E/E′-box), day-time (D-box), and night-time (Rev-Erb/ROR binding element or RRE) elements (Ueda et al., 2005). The E/E′-box-mediated transcriptional program has a critical role in the core autoregulatory loop of the mammalian circadian clock (Gekakis et al., 1998; Sato et al., 2006). In this core loop, bHLH-PAS transcriptional activators such as BMAL1 and CLOCK form heterodimers that directly and indirectly activate the transcription of their target genes, including the transcriptional repressors *Per* and *Cry*. PERs and CRYs in turn form repressor complexes that physically associate with the BMAL1/CLOCK complex to inhibit E/E′-box-mediated transcription, closing the negative feedback loop (Griffin et al., 1999; Kume et al., 1999; Okamura et al., 1999). This negative feedback, together with delayed expression of *Cry*, is critical for self-sustained circadian clock function (Hogenesch and Ueda, 2011; Ueda et al., 2005; Ukai-Tadenuma et al., 2011).

In the mammalian clock, however, transcription and translation are not the whole story; multisite phosphorylation also plays a central role (Gallego and Virshup, 2007). PER proteins undergo robust circadian changes in phosphorylation (Lee et al., 2001). Mutations in the potential phosphorylation sites of PERs or in their kinases, such as casein kinase I ε/δ (CKIε/δ), alter the circadian period (Lowrey et al., 2000; Meng et al., 2008; Toh et al., 2001; Xu et al., 2005, 2007). The oscillation period is also affected by pharmacological perturbation of CKI, CKII, or GSK3β (Chen et al., 2012; Hirota et al., 2008; Isojima et al., 2009; Meng et al., 2010; Tsuchiya et al., 2009; Walton et al., 2009). PER proteins can be phosphorylated at multiple sites by these kinases (Camacho et al., 2001; Gallego et al., 2006a; Maier et al., 2009; Schlosser et al., 2005; Takano et al., 2000; Tsuchiya et al., 2009; Vanselow et al., 2006). Furthermore, temperature-insensitive phosphorylation of a PER-derived peptide by CKIε/δ has been observed in vitro (Isojima et al., 2009). In addition to phosphorylation, the reverse reaction, dephosphorylation,

seems to play an important role in the mammalian circadian clock because the oscillation period is also affected by the pharmacological or RNA-interference-mediated perturbation of protein phosphatase 1 (PP1), which has been implicated in the dephosphorylation of PER (Gallego et al., 2006b; Lee et al., 2011; Schmutz et al., 2011) and PP5 (Partch et al., 2006).

The central role played by circadian posttranslational oscillators (PTOs) mediated by multisite phosphorylation is best understood in cyanobacteria. Purified clock proteins from the cyanobacterium *Synechococcus elongatus* can be used to reconstitute an in vitro posttranslational circadian oscillator (Johnson et al., 2008; Nakajima et al., 2005). This system contains three essential proteins: KaiA, KaiB, and KaiC. KaiC exhibits both autophosphorylation and autodephosphorylation activities; autophosphorylation is enhanced by KaiA, whereas KaiB inhibits KaiA. When the three proteins are incubated together with an excess of ATP, the phosphorylation level of KaiC oscillates with an ~24 hr period. The period of KaiC phosphorylation oscillations is fairly unaffected by the incubation temperature, suggesting that the KaiC PTO is a bona fide circadian oscillator. Studies have further shown that the phosphorylation cycle involves the sequential phosphorylation and dephosphorylation of two sites in KaiC (Nishiwaki et al., 2007; Rust et al., 2007).

It is even possible that posttranslational mechanisms might permit the mammalian circadian clock to operate in the absence of regulation by gene expression. When cultured fibroblast cells are treated with reagents that interfere with transcription, one would expect oscillations based on a TTO to be severely affected. Instead, circadian oscillations are robust to changes in transcription rate (Dibner et al., 2009). In addition, cyclic expression of *Bmal1* and *Clock* seems not to be necessary for circadian rhythmicity (von Gall et al., 2003). As for CRY, rhythmic, phase-specific expression of *Cry1* is critical for robust circadian oscillation (Ukai-Tadenuma et al., 2011), yet $Cry1^{-/-}$:$Cry2^{-/-}$ cells can exhibit weak circadian oscillations under constant expression of *Cry1* (Ukai-Tadenuma et al., 2011) or a constant supply of CRYs (Fan et al., 2007). Further evidence comes from red blood cells, which show a circadian variation in the cellular redox state despite the absence of transcription (O'Neill and Reddy, 2011). While these results do not constitute direct evidence of a posttranslational oscillator that can operate independently from transcription, they suggest that processes other than transcription and translation may be responsible for oscillations under some conditions.

One simple and attractive possibility is that, under some conditions, multisite phosphorylation systems can oscillate without additional regulation. Theoretical studies have indicated that multisite phosphorylation systems can exhibit a large number of stable states under very generic conditions (Markevich et al., 2004; Thomson and Gunawardena, 2009). Previous studies of oscillatory phosphorylation systems, such as the cyanobacterial clock (Clodong et al., 2007; Rust et al., 2007; van Zon et al., 2007), mitogen-activated protein kinase (MAPK) systems (Chickarmane et al., 2007; Liu et al., 2011; Qiao et al., 2007; Shankaran et al., 2009), and other biochemical oscillators (Ferrell et al., 2011; Kholodenko, 2006; Novák and Tyson, 2008) typically employed complex regulatory schemes. Cyanobacterial clock models (Clodong et al., 2007; Rust et al., 2007; van Zon et al., 2007) are constructed based on the autokinase and autophosphatase properties of KaiC. This unique feature makes the detailed conclusions drawn from these models difficult to apply to generic enzyme-substrate reactions. MAPK models are constructed based on a more general substrate-enzyme reaction scheme, but they often involve multiple substrates sharing an enzyme, protein synthesis, and degradation, or active feedback regulation of enzyme activity by a substrate. It is not clear whether such intricate regulation is required for oscillations, or whether a more generic system would suffice.

Here we show that autonomous, robust oscillations are possible in a system consisting of a single substrate with two phosphorylation sites. The substrate is modified by one kinase and one phosphatase, and no additional regulation is necessary. In a sense, this is the simplest possible biochemical oscillator. An extensive search of the model's parameter space reveals two design motifs for a simple biochemical oscillator. These features can be readily associated with known properties of PERs, CKIε/δ and other enzyme-substrate pairs described above. Under some conditions, the oscillation period is almost unaffected by systematic changes in the enzyme reaction rates induced by temperature differences, suggesting that temperature compensation is possible in this system. The simplicity and generality of the model make it a potentially useful design tool for de novo biochemical oscillators, and suggest that biological posttranslational oscillation may be more common than previously suspected.

RESULTS

Multisite Substrate Modifications Can Oscillate with Two Opposing Enzymes

To elucidate the minimum requirements for a PTO, we began by defining a set of components. Cyclic changes in substrate phosphorylation state require both a kinase and a phosphatase. Single-site systems will converge to a unique steady state under relevant conditions (see Extended Experimental Procedures; Figure S1), and a two-site system is the simplest one in which oscillations might be possible (Figure 1A). The model is described as a phosphorylation system, but the same results could be applied to any type of posttranslational modification. There are four distinct substrate states (Figure 1B): S_{00}, which is completely unphosphorylated; S_{01} and S_{10}, which are singly phosphorylated; and S_{11}, which is doubly phosphorylated. The same kinase (E) and phosphatase (F) act on both sites. All reactions involve a 1:1 association of enzymes and substrates, with an intermediate enzyme-substrate complex (Figure 1C). The reactions are described with the use of mass-action kinetics. Although the model equations do not explicitly assume enzyme saturation by substrate, we assumed an excess of substrate over enzyme, and enzyme-substrate binding was usually saturated.

We found that sustained oscillations could be observed in certain parameter regions (Figure 1D). After an initial transient, integrations that began under different initial conditions rapidly converged to a common trajectory with the same amplitude and period, in other words, a limit-cycle oscillation (Figure 1E).

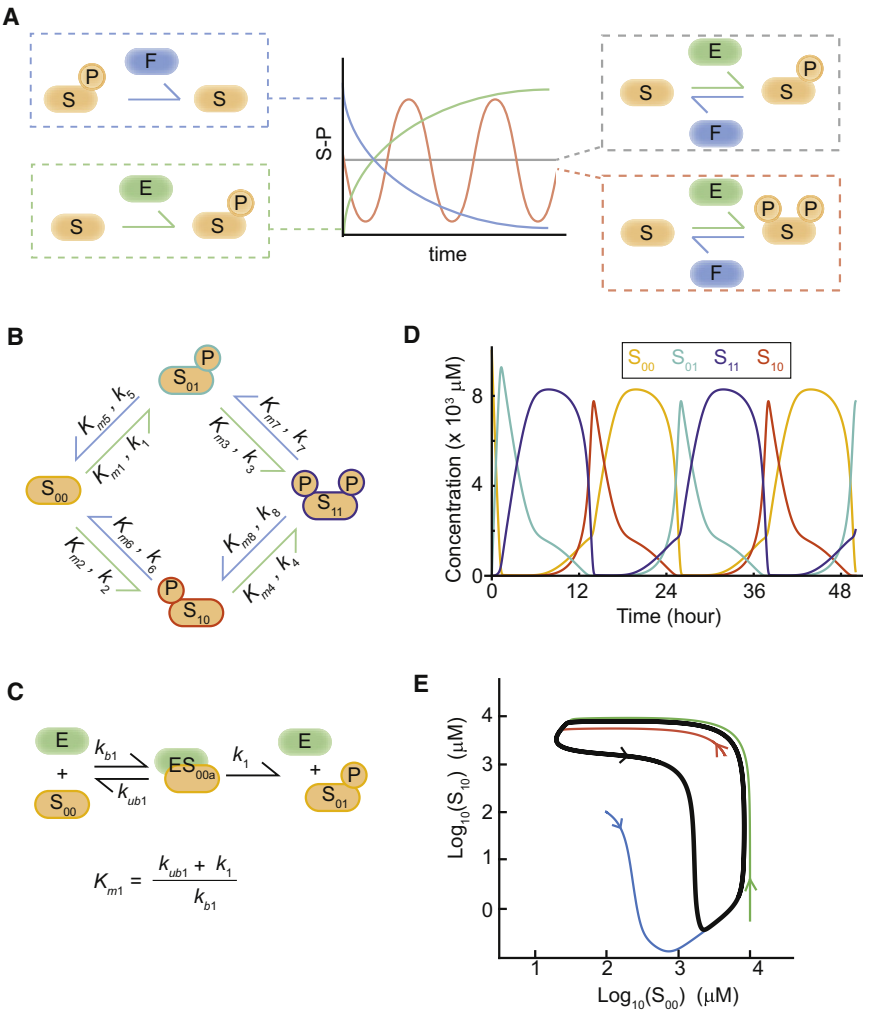

Figure 1. Multisite Substrate Modifications Can Oscillate with Two Opposing Enzymes

(A) A phosphatase (blue) or a kinase (green) acting on the substrate alone will yield monotonic convergence to a steady state, as indicated by blue and green curves. A kinase and phosphatase acting in concert are required for sustained oscillations (red).

(B) PTO reaction network. The substrate can be phosphorylated on two distinct sites, and the kinase and phosphatase act on all four phosphorylation states.

(C) Enzymatic reactions involve an intermediate enzyme-substrate complex.

(D) Time course of oscillations for an example parameter set.

(E) Oscillations projected into the S_{00}-S_{10} plane. Different initial transients (colored arrows) converge rapidly to a single limit-cycle attractor (black).

See also Figure S1.

In our system, a limit-cycle oscillation is present only when the equilibrium state is unstable.

Oscillatory Systems Possess Two Design Motifs

Once we had represented the system as a system of dynamical equations, our next aim was to determine which values of the system parameters would lead to sustained oscillations. The rate constants k_1...k_8 represent the number of substrate molecules converted to product molecules in a given reaction per enzyme per minute. The binding constants K_{m1}…K_{m8} are the substrate concentrations at which the rates of reaction 1–8 reach half of their maximum. If the binding is strong, then K_m will be low because the enzyme-substrate binding is easily saturated. This system is too large and complex for straightforward analytical study, so we chose to identify solutions numerically through an extensive search of parameter space.

We generated solutions by selecting parameters from an exponential distribution bounded to the interval 1–1,000 min^{-1} for k_1–k_8 and 0.01–1,000 μM for K_{m1}–K_{m8}. This range corresponds to reasonable values typically used to model systems such as MAPK (Chickarmane et al., 2007; Liu et al., 2011; Markevich et al., 2004; Qiao et al., 2007; Shankaran et al., 2009).

The "hit rate" of oscillating parameter sets was rather low, ~0.1%. The search was continued until ~10^6 oscillating parameter sets had been found (Figure 2A). Because this population may contain several distinct types of oscillators, we categorized the parameter sets using a clustering algorithm that accounts for the symmetry of the reaction network (see Extended Experimental Procedures). Two major clusters were present over a wide range of cluster diameters, and we chose a diameter for which these two clusters accounted for ~70% of solutions (Figures 2B and S2A). The parameter distributions for the major clusters are shown in Figure 2C. Both clusters exhibit approximate symmetry: fast and slow reactions or strong and weak binding constants tend to be located at symmetry-related positions. For example, in cluster 1, k_1, k_8, K_{m2}, and K_{m7} all tend to be high, whereas k_2, k_7, K_{m4}, and K_{m5} all tend to be low. The schematic diagrams shown in Figure 2D will be unchanged if the diagram is rotated 180° and the kinase and phosphatase are interchanged. Symmetry will rarely be exact for individual parameter sets; the symmetric pattern emerges only when a large number of parameter sets are compared.

Based on these histograms, consensus features of each major cluster can be identified (Figure 2D). Two design motifs are shared by both major clusters. The first is a unidirectional bias: in general, the rates of the "forward" (clockwise) reactions, k_1, k_3, k_6, and k_8, are higher than the corresponding "reverse" reactions, k_5, k_7, k_2, and k_4, respectively. The second is the presence of enzyme-sequestering steps. In cluster 1, the value of K_{m4} is usually low, meaning that S_{10} binds the kinase very strongly. The kinase-catalyzed $S_{10} \rightarrow S_{11}$ conversion is much slower than its reverse reaction; in this sense, the binding of the kinase by S_{10} is unproductive. Although the $S_{10} \rightarrow S_{00}$ conversion is

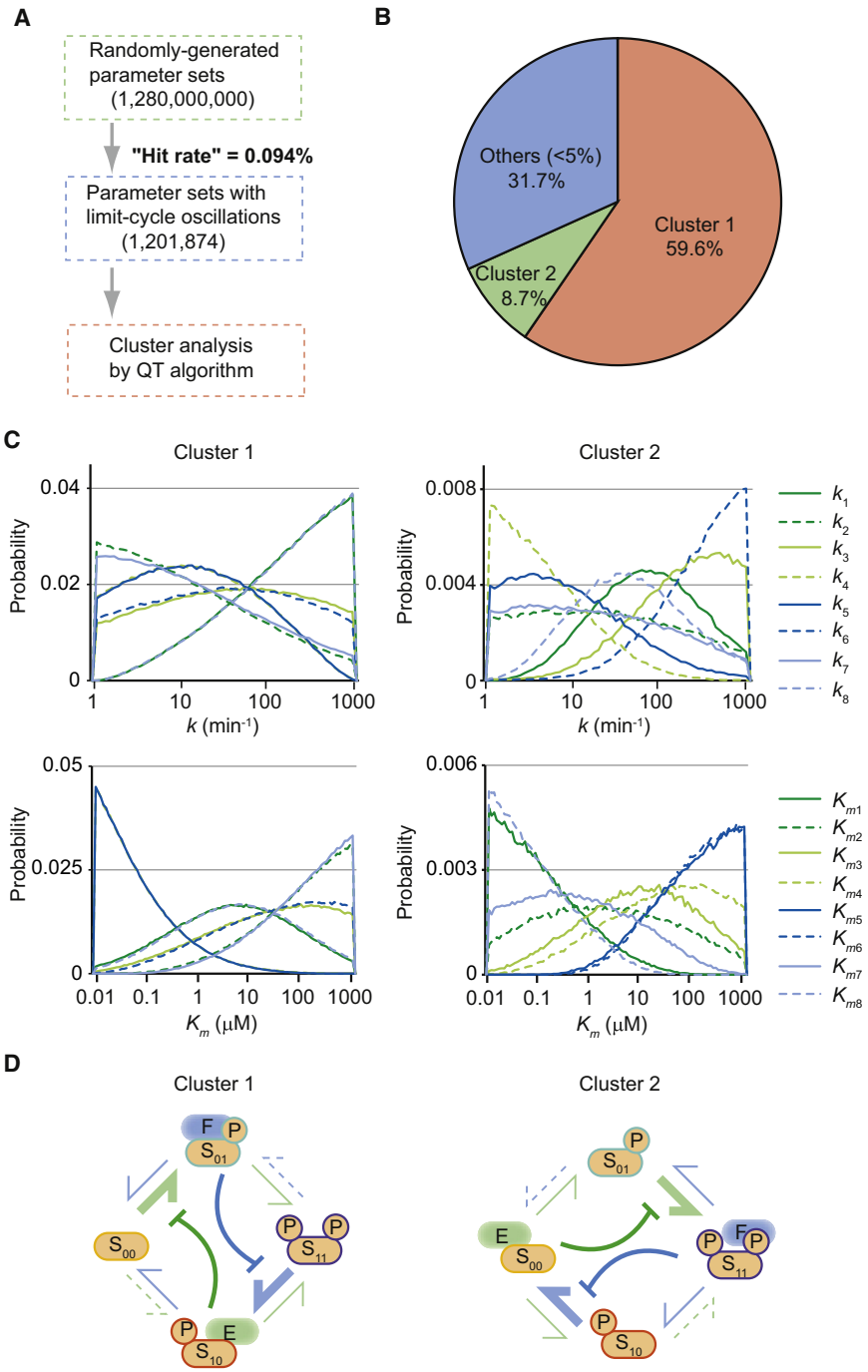

Figure 2. Oscillatory Systems Possess Two Design Motifs

(A) Workflow for motif identification.

(B) Results of QT clustering with a (unitless) diameter of 10.5.

(C) Parameter histograms for the two largest clusters. Although considerable variability exists, clear trends in rate and binding constants can be distinguished.

(D) Schematic representation of cluster motifs. Fast reactions are indicated by thick arrows; slow reactions are indicated by dotted arrows. Indirect negative regulation by enzyme sequestration is indicated by curved arrows with flat ends.

See also Figure S2.

fairly slow, it will proceed to completion because its reverse reaction ($S_{00} \rightarrow S_{10}$) is inhibited by the kinase sequestration. The next forward reaction, $S_{00} \rightarrow S_{01}$, requires the kinase and is unable to proceed until S_{10} has been depleted by conversion to S_{00}. Once the $S_{10} \rightarrow S_{00}$ reaction has gone to completion, nearly the entire substrate population will be in the S_{00} state and the kinase will no longer be sequestered by S_{10}. At this point, the kinase can bind S_{00} and the inhibited $S_{00} \rightarrow S_{01}$ reaction can proceed. In the same way, the phosphatase is sequestered by S_{01} (i.e., K_{m5} is low), inhibiting the subsequent $S_{11} \rightarrow S_{10}$ step. These sequestration steps create checkpoints that ensure that the oscillatory cycle cannot proceed until one substrate state has been depleted and most of the substrate population has moved into the subsequent state.

The situation in cluster 2 is only slightly different. A low value of K_{m1} means that S_{00} binds the kinase strongly. Unlike the unproductive S_{10}-kinase complex, this complex is involved in a forward reaction and leads to the production of S_{01}. The subsequent kinase-catalyzed $S_{01} \rightarrow S_{11}$ reaction, however, cannot proceed until S_{00} has been depleted, resulting in a checkpoint that requires nearly the entire population to accumulate as S_{01}. The low value of K_{m8} means that the phosphatase is sequestered by S_{11}, and therefore most of the population has to accumulate as S_{10} before the $S_{10} \rightarrow S_{00}$ step can proceed.

The remaining small clusters (~30% of the total) are generally similar to either cluster 1 or cluster 2. If all parameter sets assigned to neither cluster 1 nor cluster 2 are grouped together, their parameter distribution is similar to that of cluster 1 or cluster 2. For example, Figure S2B shows both cluster-2-type characteristics (high k_3 and k_6, low k_4 and k_5, and low K_{m1} and K_{m8}) and cluster-1-type characteristics (high k_1 and k_8, low k_2 and k_7, and low K_{m4} and K_{m5}). To a first approximation, therefore, solutions can be categorized as being similar to either cluster 1 or cluster 2. The presence of two distinct oscillatory clusters in parameter space can also be confirmed by principal components analysis (PCA) (Figures S2C and S2D).

To summarize, an extensive search of the 16-dimensional parameter space revealed two types of oscillatory parameter

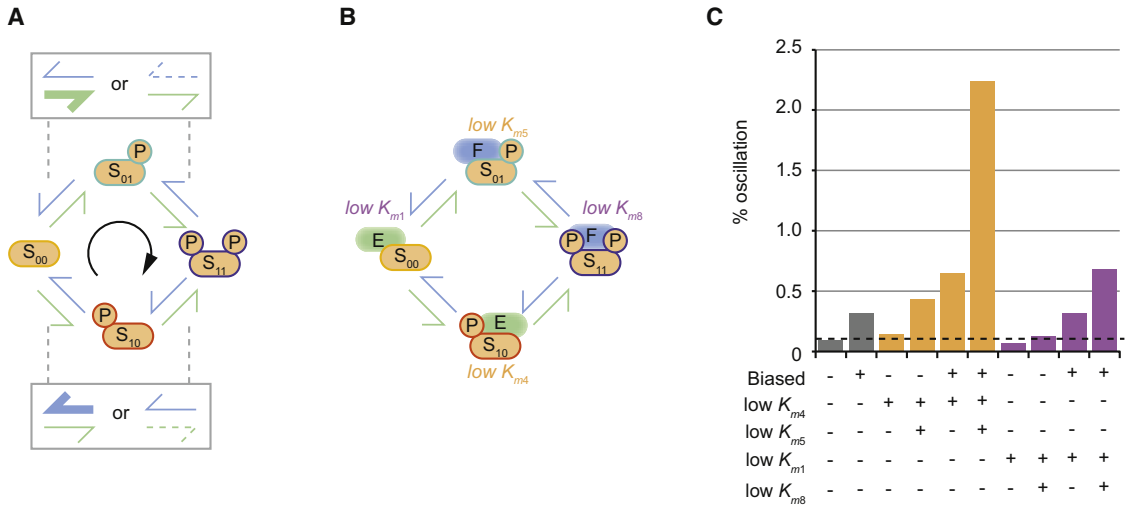

Figure 3. Functional Significance of Two Design Motifs

(A) Unidirectional modification cycle. Clockwise reactions are faster than counterclockwise ones, leading the system to prefer the ordering S_{00},S_{01},S_{11},S_{10},S_{00}….

(B) Indirect negative regulation by enzyme sequestration.

(C) Imposing the strong binding associated with enzyme sequestration during the random parameter search results in modest gains in the oscillator discovery rate. If this constraint is combined a clockwise rate constant bias, the discovery rate rises substantially.

See also Figure S3.

sets, illustrated in Figure 2D. Based on their parameter distributions, we have proposed two design motifs: a unidirectional bias of catalytic rate constants and indirect negative regulation through enzyme sequestration.

Functional Significance of Two Design Motifs

The random-search results surely contain a large number of statistical correlations. How then can we determine whether the design motifs described above actually promote oscillation? One approach is to begin with a design motif and use it to constrain the search process (Figures 3A and 3B). If an alleged motif helps to improve the rate of oscillator discovery, then it is functionally significant. Enforcing a clockwise bias in the rate constants, for example, increases the hit rate 3.4-fold (Figure 3C). Constraining the search such that K_{m4} is low improves the success rate 1.5-fold. If both constraints are combined, a 6.8-fold increase is achieved. Requiring both K_{m4} and K_{m5} to be low and maintaining the rate constant bias enforces the entire cluster 1 pattern; this gives an oscillator discovery rate that is 23.6 times the unbiased value. Qualitatively similar results can be obtained for cluster 2. Requiring a low value for K_{m1} fails to improve the success rate, but combining constraints on K_{m1} and/or K_{m8} with the rate constant bias yields significant improvement.

Parameter histograms similar to those in Figure 2C were also constructed from the constrained search results (Figure S3). Although only part of the cluster 1 pattern was enforced (clockwise bias and low K_{m4}), the complete pattern was often present. For example, constraining K_{m4} to be low resulted in a low value for K_{m5}, and the distributions of the catalytic rate constants are similar to those seen in Figure 2C. Although the distribution for K_{m5} is broader than the distribution imposed for K_{m4}, and the presence of two strong sequestration motifs is not absolutely essential for oscillations, it is clear that oscillations are far more probable with both motifs present than with only one present.

Although the identification of design motifs from unbiased random search results can be somewhat subjective, the "inverse analysis" presented in this section shows that the motifs identified are functionally significant. Not only are unidirectional bias and enzyme sequestration typically present in oscillating parameter sets, demanding their presence also increases the number of oscillators found.

Period- and Amplitude-Determining Processes

Once we had identified oscillator-enriched regions of the parameter space, we aimed to determine which specific parameters have a strong impact on system properties, in particular the oscillation period and amplitude. In Figure 4A, an example of a symmetric cluster 1 (see Table S1) is used as the reference parameter set for bifurcation calculations (Strogatz, 1994). The bifurcation diagrams in Figures 4A and S4A show the equilibrium points (either stable or unstable) of the system, as well as the period and amplitude of oscillations when they exist. Similar bifurcation methods can also be used to characterize the robustness of the oscillations (Figure S4B; Extended Experimental Procedures).

The slow steps by which the enzyme-sequestering substrate states are depleted can be expected to have a large effect on the period. The bifurcation diagram for k_3 confirms this intuition. Although the impact of k_3 on the oscillation amplitude is minimal, decreasing k_3 causes the period to increase dramatically, until oscillations terminate in a Hopf bifurcation at $k_3 \cong 7 \times 10^{-4}$ (Figure 4A). Figure 4B illustrates the impact of k_3 on period determination. When k_3 is reduced by half, the transition phase from S_{01} to S_{11} (yellow-shaded) nearly doubles.

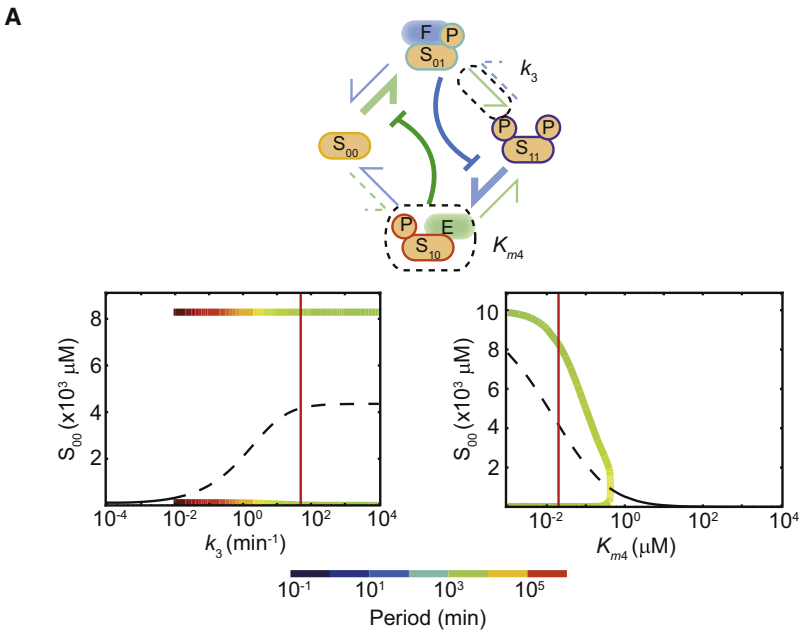

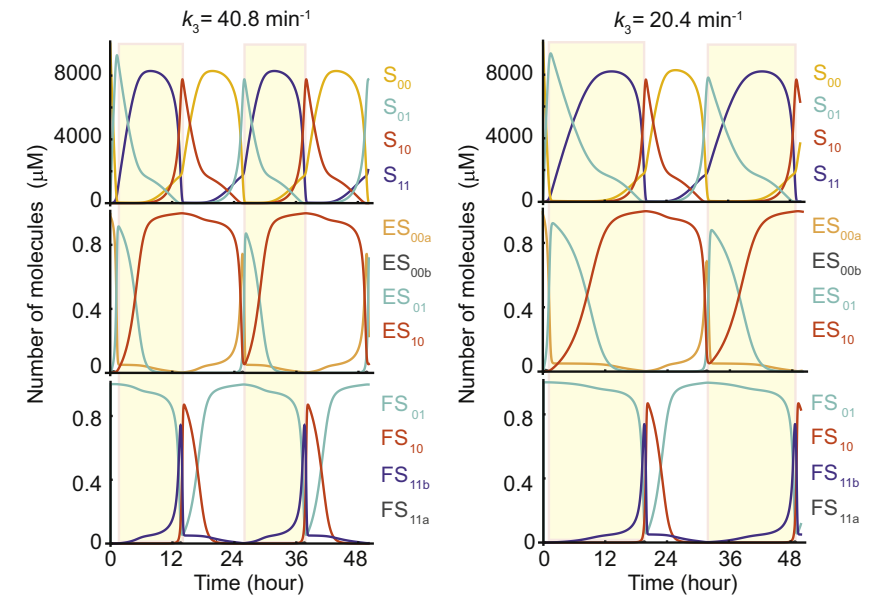

Figure 4. Period- and Amplitude-Determining Processes

(A) Two examples of single-parameter bifurcation diagrams. Solid black lines denote stable fixed points, and dashed black lines indicate an unstable fixed point surrounded by a limit cycle. Red vertical lines denote the parameter value in the symmetric example set; see Table S1 for precise values. Colored lines show oscillation extrema, with the period indicated by the line color; k_3 has a dramatic effect on the period, whereas K_{m4} primarily affects the amplitude. A more extensive set of bifurcation diagrams is shown in Figure S4.

(B) Effects of decreasing a single rate constant. The oscillation cycle is divided roughly into two halves: the net conversion of S_{10} to S_{01} (via S_{00}) is shown on a white background, and the net conversion of S_{01} to S_{10} (via S_{11}) is shown on a shaded background. In the symmetric case (left), these phases are of equal length. If k_3 (the rate constant for the slow $S_{01} \rightarrow S_{11}$ conversion) is halved, the length of the $S_{01} \rightarrow S_{11} \rightarrow S_{10}$ phase (shaded background) nearly doubles, indicating that the reaction with rate k_3 is rate limiting for this phase. See also Figure S4 and Table S1.

K_{m4}, the binding constant of kinase to S_{10}, can be decreased apparently without limit, whereas the maximum oscillatory value of K_{m4} is limited by a supercritical Hopf bifurcation (Figure 4A). Tight binding of the kinase by S_{10} (and of the phosphatase by S_{01}) is an important part of the design motif described above, and the loss of sequestration rapidly abolishes oscillations.

Robustness of the Oscillation Period against Stochastic Fluctuations

The mass-action approach assumes that chemical concentrations are continuous variables that can take on any positive value. At typical cellular volumes and concentrations, however, the discrete nature of molecules may be important and a stochastic approach becomes necessary. Stochastic simulations also allow us to quantify the robustness of oscillations against internal noise. Noise tolerance is an important requirement for realistic biological models.

The results of stochastic simulations for cluster 1 are shown in Figure 5 (see Table S2; similar plots for cluster 2 are shown in Figures S5A and S5B). For 600 molecules of each type of enzyme (maintaining the concentrations used above for a cell-like volume of 10^{-15} L), the oscillations are extremely robust. As the system shrinks (i.e., the total number of molecules decreases), the oscillator runs slowly relative to the deterministic limit (Figures 5A, S5C, and S5D; see also Extended Experimental Procedures). Even when only one of each type of enzyme was present, the period length was surprisingly robust (the standard deviation of the oscillation period was ~2% of the mean period). These results suggest that our model system is fairly robust to the internal noise that will prevail at the cellular scale.

Coupling of Single-Molecule Oscillators Is a Design Principle

Further insight can be gained by tracking the state of individual molecules. Figure 5B shows the results of stochastic simulations. The top panels show the bulk population behavior, and the middle panels show smoothed trajectories of the four

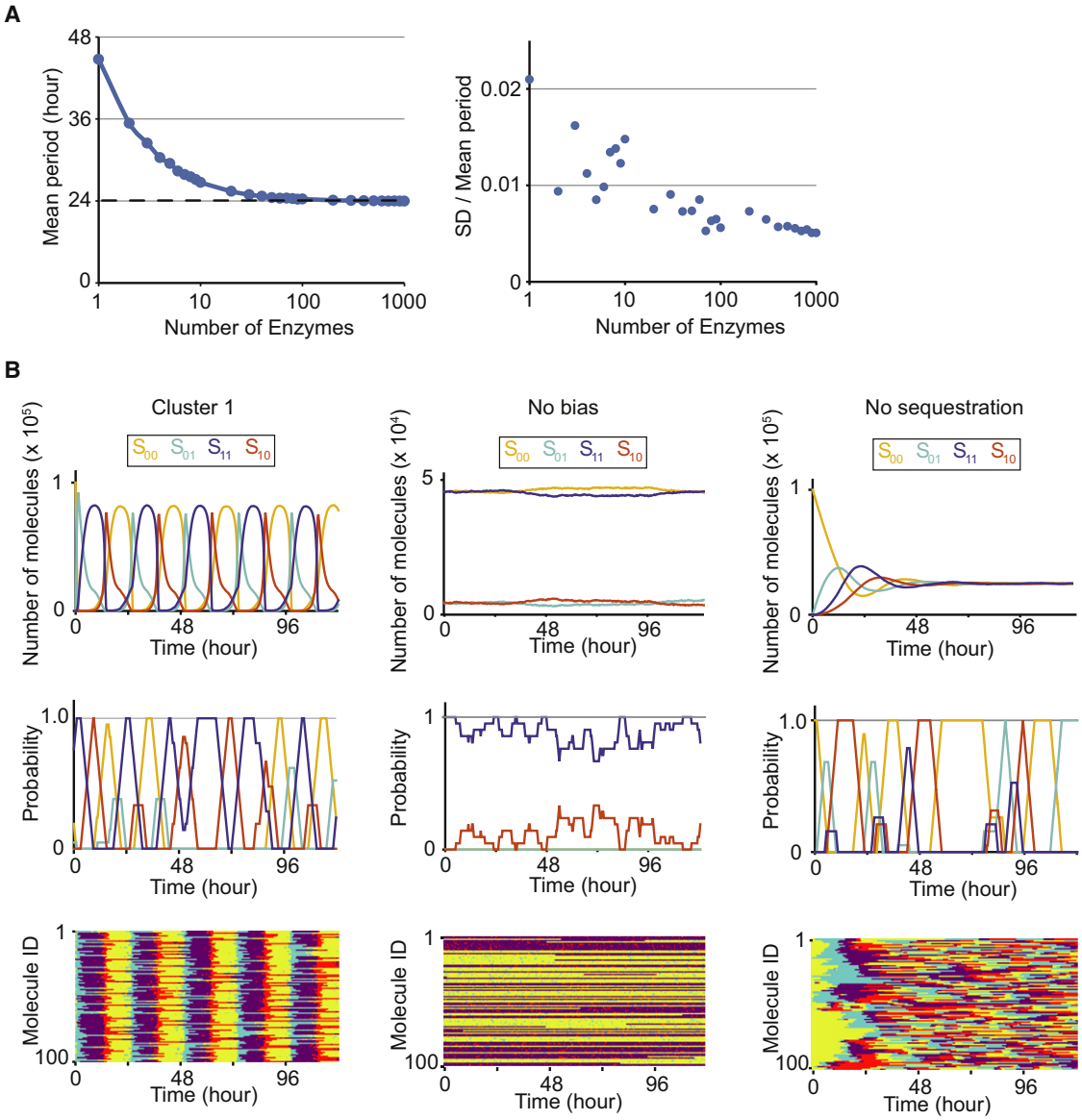

Figure 5. Coupling of Single-Molecule Oscillators Is a Design Principle

(A) Robustness of the oscillation period against stochastic fluctuations. Low-copy-number oscillations are slow (left) and variable (right) relative to larger systems. In the continuous limit, the period is precisely 24 hr with zero variability.

(B) Top row: Plots of the bulk population for the cluster 1 oscillator (left), similar binding constants lacking a rate constant bias (middle), and similar rate constants with a clockwise bias but no sequestration (right). Middle row: Smoothed traces showing the state of a single (arbitrarily chosen) substrate molecule. Bottom row: Results for 100 individually tracked molecules, each shown as a horizontal raster line, color-coded as in the plots above. If synchronization by enzyme sequestration is removed, the substrates still act as single-molecule oscillators but lack population-level coherence. If the unidirectional rate constant bias is eliminated, the substrates become trapped and fail to progress around the cycle. See also Figure S5 and Table S2.

phosphorylation states of an arbitrarily chosen substrate molecule. In the bottom panels of Figure 5B, each row of pixels represents a single substrate molecule, and different colors represent the four phosphorylation states.

The middle panel of the "Cluster 1" column (Figure 5B) shows cyclic transitions among the four phosphorylation states. Each individual substrate molecule acts as a noisy oscillator, synchronized with the rest of the population. In addition, the bottom panel of the Cluster 1 column indicates clear bands of S_{11} (blue) and S_{00} (yellow) dominance; individual substrates experience S_{01} (cyan) transiently during the transition into the S_{11} band, and S_{10} (red) during the transition into the S_{00} band. Also note that the $S_{00} \rightarrow S_{01}$ and $S_{11} \rightarrow S_{10}$ transitions seem fairly sharp, whereas the $S_{10} \rightarrow S_{00}$ and $S_{01} \rightarrow S_{11}$ transitions are more diffuse. This suggests that the population is coupled at the $S_{00} \rightarrow S_{01}$ and $S_{11} \rightarrow S_{10}$ transitions, where they are

synchronized by enzyme sequestration. The same is true for sequestration of phosphatase by S_{01}.

We next observed single-molecule behaviors when either one of the two design motifs was removed. When the unidirectional motif was removed (by setting k_1–k_8 equal but maintaining binding affinities), the individual substrate molecules no longer cycled through phospho-states in a defined order (the "No bias" column). When the sequestration motif was removed (by setting all binding affinities equal), phospho-state transitions failed to synchronize (the "No sequestration" column). Although the bulk population converged to a stable fixed point, individual substrate molecules still transitioned between phospho-states in a defined order (middle and bottom panels). These results confirm that (1) the design motif of unidirectional modification cycle constitutes a single-molecule oscillator, and (2) the design motif of enzyme sequestration serves to synchronize noisy single-molecule oscillators, suggesting that coupling of single-molecule oscillators is a design principle.

The Period of a Simple PTO Can Be Temperature Compensated

To qualify as a bona fide circadian clock, an ~24 hr cellular rhythm must also exhibit temperature compensation, meaning that the oscillation period is fairly robust to changes in temperature. The temperature coefficient Q_{10} measures the factor by which a process accelerates when the temperature is raised by 10°C. Typical Q_{10} values for biochemical reactions range from 2 to 3; measured values for circadian clocks range from 0.8–1.4 (Dunlap et al., 2003).

In our model system, one can calculate Q_{10} values for the oscillation period by assuming temperature coefficients $Q_{10}^{(E)}$ and $Q_{10}^{(F)}$ for the kinase and phosphatase, and rescaling the rate constants in accordance with a given temperature change (Extended Experimental Procedures; Figures 6A and S6A–S6C). $Q_{10}^{(E)}$ and $Q_{10}^{(F)}$ do not uniquely determine the oscillation Q_{10} ($Q_{10}^{(cycle)}$); by analyzing a large number of parameter sets, one can calculate a histogram of Q_{10} values (Figure 6B). In general, larger values of $Q_{10}^{(E)}$ and $Q_{10}^{(F)}$ cause the peak of $Q_{10}^{(cycle)}$ to be shifted to higher values, and the width of the $Q_{10}^{(cycle)}$ distribution increases with the difference between $Q_{10}^{(E)}$ and $Q_{10}^{(F)}$. We considered the case with $Q_{10}^{(E)} = 1$ and $Q_{10}^{(F)} = 3$, corresponding to a temperature-insensitive kinase (such as CKIε/δ; Isojima et al., 2009) and a typical phosphatase. The resulting histogram includes populations that are strongly undercompensated ($Q_{10} >> 1$) as well as some that are overcompensated ($Q_{10} < 1$; Figure 6C).

Different degrees of temperature sensitivity correlate with changes in the distribution of individual parameters (Figures 6D, S6D, and S6E). In general, undercompensated oscillators will have higher rates for the temperature-insensitive kinase reactions and lower rates for the temperature-sensitive phosphatase reactions, such that the rate-determining steps are strongly affected by temperature. For well-compensated oscillators, the opposite is true (Figure 6E), and temperature compensation can be observed even in stochastic simulations (Figure 6F; Table S3). See the Extended Experimental Procedures for a more extensive discussion of this issue.

DISCUSSION

General Applicability of a Design Principle Composed of Two Design Motifs

Although the model developed in this study is very simple, we can extract a design principle of wider applicability. Two design motifs appear to be required for robust oscillations (Figure 7A). The first is a well-defined ordering of phosphorylation states, in which the rate constants in the forward direction around the loop are (in general) faster than those in the reverse direction. The other design motif is the presence of synchronizing checkpoints at which single-molecule oscillators that have progressed more quickly must stop and wait for the others. This is accomplished by enzyme sequestration: the cycle cannot proceed past a checkpoint until a strong-binding substrate population has been sufficiently depleted to permit competing reactions.

The general design principles uncovered in this study can also be applied to situations in which more than two phosphorylation sites or more than one kinase (and phosphatase) are present (Figure 7B). The principle may be also conserved when protein degradation and synthesis are incorporated in an appropriate position: if a substrate acts as a repressor for its own transcription and is degraded depending on phosphorylation, then such a transcription-degradation pathway will be compatible with the role of phosphatase reaction (i.e., the disappearance of phosphorylated substrate will lead to the appearance of unphosphorylated substrate; Figure 7C; Extended Experimental Procedures).

In this study we considered the behavior of an isolated PTO; oscillators in real biological systems are responsive to external signals that can modify their behavior. In this context, the relationship of our model to "integrators" (which accumulate a response to incoming signals) and "resonators" (which respond preferentially to signals with a given frequency) may be an interesting avenue for future study (Conrad et al., 2008; Guantes and Poyatos, 2006).

Two Design Motifs Are Present in the Natural Circadian Clocks

The design principle mentioned above can easily be related to known properties of substrates and enzymes involved in circadian clock systems. In the cyanobacterial clock, the phosphorylation states of the clock protein KaiC have a well-defined cyclic order (Nishiwaki et al., 2007; Rust et al., 2007), similar to the first design motif (unidirectional modification cycle) in our model. In higher eukaryotes, CKIε/δ predominantly phosphorylates the consensus sequence pS-x-x-S*, where pS is a phosphorylated serine, x can be any amino acid, and S* is the target serine (Flotow et al., 1990). This motif promotes ordered phosphorylation: if the substrate contains a pS-x-x-S-x-x-S sequence, CKIε/δ will tend to phosphorylate the second serine before the third. In mammalian PER proteins, contiguous S-x-x-S motifs have been shown to be important for period determination (Toh et al., 2001; Vanselow et al., 2006; Xu et al., 2007).

For the second motif (enzyme sequestration), tight binding between the enzyme and substrate is required. Tight enzyme-substrate binding is found in several enzymes involved in circadian clock systems. In mammals, CKIε/δ forms a stable complex

Cell PRESS
Open ACCESS

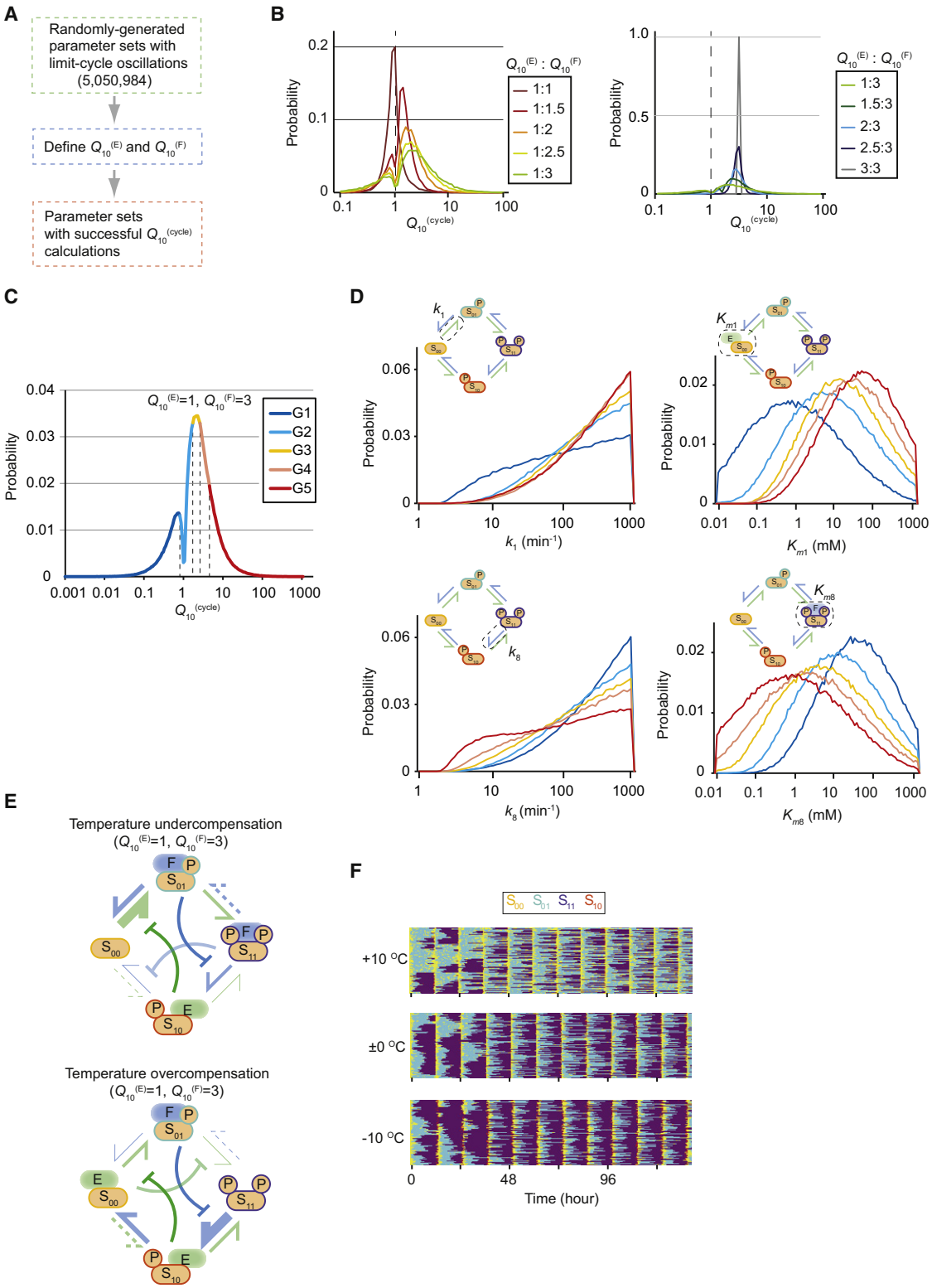

Figure 6. The Period of a Simple PTO Can Be Temperature Compensated

(A) Workflow diagram.

(B) Histogram of $Q_{10}^{(cycle)}$ values with different combinations of $Q_{10}^{(E)}$ and $Q_{10}^{(F)}$; Q_{10} for binding/unbinding reactions is assumed to be 3.0 for all calculations.

(C) Histogram of $Q_{10}^{(cycle)}$ values when $Q_{10}^{(E)}$ = 1, $Q_{10}^{(F)}$ = 3. Parameter sets were separated into one of five groups depending on their degree of temperature overcompensation (blue) or undercompensation (red).

with PERs that is important for clock function (Akashi et al., 2002; Camacho et al., 2001; Lee et al., 2004; Vielhaber et al., 2000). PP1 also interacts strongly with PERs (Gallego et al., 2006b). It is not known whether these tight bindings serve to synchronize substrates in different phases of an oscillation cycle, but both experimental and theoretical studies have highlighted enzyme sequestration as a source of nonlinearity in biochemical reactions (Blüthgen et al., 2006; Legewie et al., 2006, 2007; Markevich et al., 2004).

Comparison with Other PTO Models

The design motifs uncovered in this study can also be seen in other mathematical models of PTOs. MAPK is typically modeled as a two-site system with strictly sequential phosphorylation, such that only three states exist (Huang and Ferrell, 1996; Kholodenko, 2000; Markevich et al., 2004). Feed-forward inhibition interactions similar to those described in this study can generate bistability, but oscillations require larger cascades or feedback loops. The cyanobacterial circadian clock has also been modeled extensively (Clodong et al., 2007; Hatakeyama and Kaneko, 2012; Rust et al., 2007; van Zon et al., 2007). These models also tend to converge on design features similar to ours, in that they typically employ some mechanism (often involving conformational changes or complex formation) to ensure that individual KaiC hexamers visit phosphorylation states in a well-defined order, and the oscillations of the individual hexamers are synchronized through competition for a limited pool of KaiA. A more detailed examination of individual models can be found in the Extended Experimental Procedures.

Although previous studies generally focused on correctly reproducing the behavior of a specific experimentally characterized system, here we focused on mapping out possible behaviors for a very general system. It is therefore quite striking that our approach, which began with no constraining assumptions about what kind of design features should promote oscillation, should lead to fairly similar conclusions.

Strategies for Experimental Validation

Our modeling results can inform the design or discovery of PTOs in several ways. No unusual substrate properties are necessary, so a simple substrate, such as a short peptide, might be adequate.

The low probability of finding oscillations in our nonbiased search may raise questions about the feasibility of discovering PTOs experimentally. Results from the constrained-parameter search, however, show that one can increase the probability >20-fold by requiring sequential (de)phosphorylation and tight enzyme-substrate binding. These features are likely to be implemented (at least in part) in substrates and enzymes found in natural oscillatory systems. Accordingly, as a starting point for experimental investigation, CKIε/δ, a PER-derived peptide, and an appropriate phosphatase might be a suitable ex vivo PTO.

CONCLUSIONS

This study illustrates the potential for robust oscillations to exist in a very simple kinase-phosphatase reaction system. This requires two design motifs: a well-ordered sequence of phosphorylation states and synchronization by enzyme sequestration. Although the vast majority of possible parameter sets examined here did not result in sustained oscillations, we were able to construct a typical example of an oscillatory parameter set with reaction rates and binding constants that were within a reasonable range for polypeptide kinases. The ultimate test of the utility of this proposed model, "proof by synthesis," lies ahead.

EXPERIMENTAL PROCEDURES

Modeling the PTO with Two Phosphorylation Sites

The PTO can be described using a system of 14 coupled ordinary differential equations (ODEs) describing the concentrations of four substrate phosphoforms, eight substrate-enzyme complexes, and two unbound enzymes (Figure 1B; the full system of equations is presented in Extended Experimental Procedures). In the case of branching reactions (e.g., phosphorylation of S_{00} to form either S_{01} or S_{10}), it is assumed that two different types of enzyme-substrate complexes are formed (ES_{00a} or ES_{00b}, respectively), consistent with the presence of two distinct phosphorylation sites on the substrate molecule. Calculations were also performed with the opposite assumption (a single complex ES_{00} that can lead to either S_{01} or S_{10}), and the results were qualitatively similar (Figure S1).

Biased Parameter Search

When a forward bias in the rate constants was desired (Figure 3), numbers were selected from the exponential distribution two at a time, with the larger number being assigned to a forward (clockwise) reaction (k_1, k_3, k_6, or k_8) and the smaller number assigned to the corresponding reverse (counterclockwise) reaction (k_5, k_7, k_2, or k_4, respectively; Figure 3A). Enzyme sequestration was encouraged by selecting constrained binding constants from an exponential distribution over 0.01–0.05 μM rather than 0.01–1,000 μM (Figure 3B).

Defining "Typical" Parameter Sets

A stereotypical example was generated for each of the dominant clusters; the parameter values chosen are listed in Table S1, and oscillations for the cluster 1 example are depicted in Figure 4A. These example clusters were designed to exhibit symmetry, so that $k_i = k_j$ and $K_{mi} = K_{mj}$ for $(i,j) \in \{(1,8),(2,7),(3,6),(4,5)\}$. Rate constants were scaled to ensure an oscillation period of 24 hr.

Bifurcation Analysis

Beginning from these stereotypical parameter sets, each parameter was systematically varied beyond the range of values over which oscillations are possible, and concentrations at the fixed points and the oscillation extrema were calculated. Although the starting parameter sets were symmetric, this symmetry was not maintained during bifurcation calculations. Note that, because of symmetry, bifurcation calculations were needed for only half of the parameters. For example, the diagram for k_8 can be obtained by

(D) Examples of parameter histograms for different oscillator groups, color-coded as in (C). The parameters k_1 and k_8 are located at symmetric positions in the network (Figure 1B) and would be equivalent if the roles of kinase and phosphatase were interchanged.
(E) Schematic diagrams of the extremes of temperature sensitivity. In the undercompensated case (top) the rate-limiting steps are catalyzed by the temperature-sensitive phosphatase, whereas in the overcompensated case (bottom) the temperature-insensitive kinase steps are rate limiting.
(F) Stochastic simulation results for a particular temperature-compensated parameter set.
See also Figure S6 and Table S3.

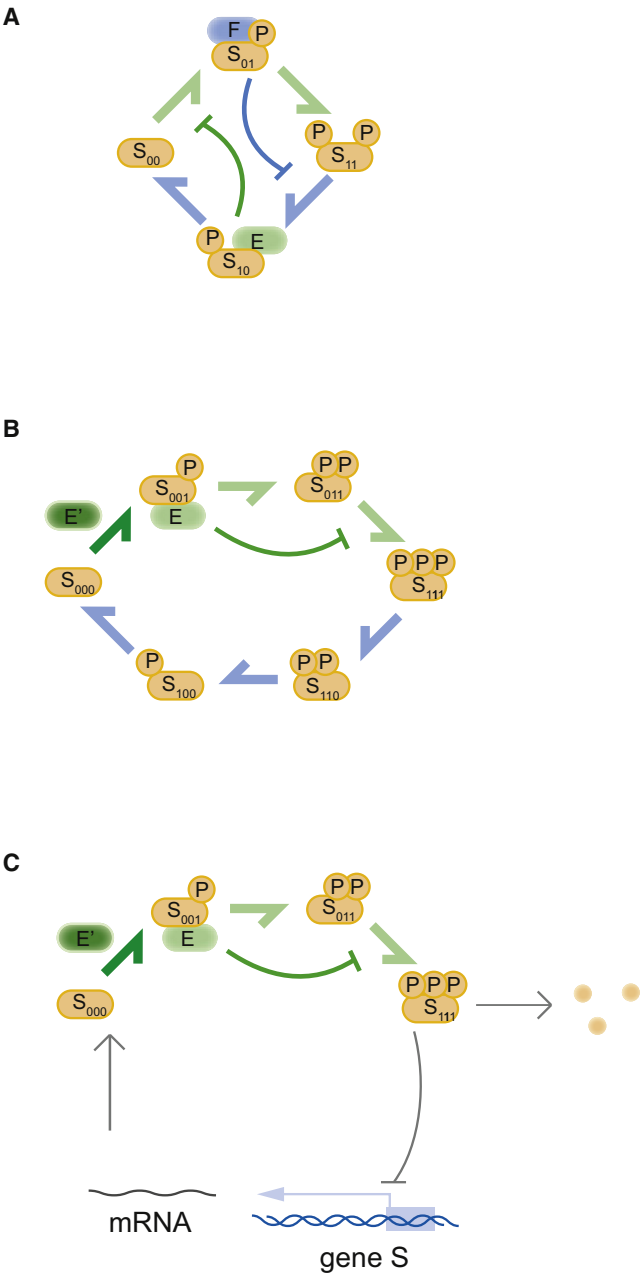

Figure 7. Generalizations of the PTO Model

(A) Simplified view of the PTO model examined in this work.

(B) The mechanisms outlined in this work could be realized in a more complex system with a larger number of phosphorylation states and more than two enzymes.

(C) Similar considerations could apply in a case in which the dephosphorylation of highly phosphorylated substrate is replaced by coupled processes of degradation and gene expression.

exchanging S_{00} with S_{11} and S_{01} with S_{10} in the k_1 calculation; the bifurcation points and period dependence will be identical.

Stochastic Simulation

We studied the reaction networks using the stochastic simulation algorithm (Gillespie, 1977) as implemented in SPPARKS (Plimpton et al., 2009). To monitor the behavior of individual substrate molecules, we modified the stochastic simulations so that in addition to a large pool of "ordinary" substrate molecules, the system contains a smaller number of "labeled" substrate molecules whose progression through the four phosphorylation states can be tracked. The interactions of the four phospho-forms of these labeled substrate molecules with the kinase and phosphatase are identical to their unlabeled counterparts, but each can be followed in the stochastic simulation as a separate molecular population, allowing us to observe how a single substrate molecule experiences the oscillatory cycle.

SUPPLEMENTAL INFORMATION

Supplemental Information includes Extended Experimental Procedures, six figures, and three tables and can be found with this article online at http://dx.doi.org/10.1016/j.celrep.2012.09.006.

LICENSING INFORMATION

ACKNOWLEDGMENTS

We thank Drs. Tatsuo Shibata and Ryokichi Tanaka for valuable comments. C.C.J. was supported by the RIKEN Foreign Postdoctoral Researcher Program. Large-scale calculations used the RIKEN Integrated Cluster of Clusters. This research was supported by an intramural Grant-in-Aid from the RIKEN Center for Developmental Biology and the Quantitative Biology Center (H.R.U.), the Uehara Memorial Foundation (H.R.U.), the Mitsubishi Foundation (H.R.U.), the President's Fund from RIKEN (H.R.U.), and a Grant-in-Aid for Scientific Research on Innovative Areas (No. 3306) from the Ministry of Education, Culture, Sports, Science, and Technology, Japan (H.R.U.).

Received: June 11, 2012
Revised: August 22, 2012
Accepted: September 8, 2012
Published online: October 18, 2012

REFERENCES

Akashi, M., Tsuchiya, Y., Yoshino, T., and Nishida, E. (2002). Control of intracellular dynamics of mammalian period proteins by casein kinase I epsilon (CKIepsilon) and CKIdelta in cultured cells. Mol. Cell. Biol. *22*, 1693–1703.

Blüthgen, N., Bruggeman, F.J., Legewie, S., Herzel, H., Westerhoff, H.V., and Kholodenko, B.N. (2006). Effects of sequestration on signal transduction cascades. FEBS J. *273*, 895–906.

Camacho, F., Cilio, M., Guo, Y., Virshup, D.M., Patel, K., Khorkova, O., Styren, S., Morse, B., Yao, Z., and Keesler, G.A. (2001). Human casein kinase Idelta phosphorylation of human circadian clock proteins period 1 and 2. FEBS Lett. *489*, 159–165.

Chen, Z., Yoo, S.H., Park, Y.S., Kim, K.H., Wei, S., Buhr, E., Ye, Z.Y., Pan, H.L., and Takahashi, J.S. (2012). Identification of diverse modulators of central and peripheral circadian clocks by high-throughput chemical screening. Proc. Natl. Acad. Sci. USA *109*, 101–106.

Chickarmane, V., Kholodenko, B.N., and Sauro, H.M. (2007). Oscillatory dynamics arising from competitive inhibition and multisite phosphorylation. J. Theor. Biol. *244*, 68–76.

Clodong, S., Dühring, U., Kronk, L., Wilde, A., Axmann, I., Herzel, H., and Kollmann, M. (2007). Functioning and robustness of a bacterial circadian clock. Mol. Syst. Biol. *3*, 90.

Conrad, E., Mayo, A.E., Ninfa, A.J., and Forger, D.B. (2008). Rate constants rather than biochemical mechanism determine behaviour of genetic clocks. J. R. Soc. Interface *5*(*Suppl 1*), S9–S15.

Dibner, C., Sage, D., Unser, M., Bauer, C., d'Eysmond, T., Naef, F., and Schibler, U. (2009). Circadian gene expression is resilient to large fluctuations in overall transcription rates. EMBO J. *28*, 123–134.

Dibner, C., Schibler, U., and Albrecht, U. (2010). The mammalian circadian timing system: organization and coordination of central and peripheral clocks. Annu. Rev. Physiol. *72*, 517–549.

Dunlap, J.C. (1999). Molecular bases for circadian clocks. Cell *96*, 271–290.

Dunlap, J.C., Loros, J.J., and Decoursey, P.J. (2003). Chronobiology: Biological Timekeeping, First Edition (Sunderland, MA: Sinauer Associates).

Fan, Y., Hida, A., Anderson, D.A., Izumo, M., and Johnson, C.H. (2007). Cycling of CRYPTOCHROME proteins is not necessary for circadian-clock function in mammalian fibroblasts. Curr. Biol. *17*, 1091–1100.

Ferrell, J.E., Jr., Tsai, T.Y., and Yang, Q. (2011). Modeling the cell cycle: why do certain circuits oscillate? Cell *144*, 874–885.

Flotow, H., Graves, P.R., Wang, A.Q., Fiol, C.J., Roeske, R.W., and Roach, P.J. (1990). Phosphate groups as substrate determinants for casein kinase I action. J. Biol. Chem. *265*, 14264–14269.

Gallego, M., and Virshup, D.M. (2007). Post-translational modifications regulate the ticking of the circadian clock. Nat. Rev. Mol. Cell Biol. *8*, 139–148.

Gallego, M., Eide, E.J., Woolf, M.F., Virshup, D.M., and Forger, D.B. (2006a). An opposite role for tau in circadian rhythms revealed by mathematical modeling. Proc. Natl. Acad. Sci. USA *103*, 10618–10623.

Gallego, M., Kang, H., and Virshup, D.M. (2006b). Protein phosphatase 1 regulates the stability of the circadian protein PER2. Biochem. J. *399*, 169–175.

Gekakis, N., Staknis, D., Nguyen, H.B., Davis, F.C., Wilsbacher, L.D., King, D.P., Takahashi, J.S., and Weitz, C.J. (1998). Role of the CLOCK protein in the mammalian circadian mechanism. Science *280*, 1564–1569.

Gillespie, D.T. (1977). Exact stochastic simulation of coupled chemical reactions. J. Phys. Chem. *81*, 2340–2361.

Griffin, E.A., Jr., Staknis, D., and Weitz, C.J. (1999). Light-independent role of CRY1 and CRY2 in the mammalian circadian clock. Science *286*, 768–771.

Guantes, R., and Poyatos, J.F. (2006). Dynamical principles of two-component genetic oscillators. PLoS Comput. Biol. *2*, e30.

Hastings, J.W., and Sweeney, B.M. (1957). On the mechanism of temperature independence in a biological clock. Proc. Natl. Acad. Sci. USA *43*, 804–811.

Hatakeyama, T.S., and Kaneko, K. (2012). Generic temperature compensation of biological clocks by autonomous regulation of catalyst concentration. Proc. Natl. Acad. Sci. USA *109*, 8109–8114.

Hirota, T., Lewis, W.G., Liu, A.C., Lee, J.W., Schultz, P.G., and Kay, S.A. (2008). A chemical biology approach reveals period shortening of the mammalian circadian clock by specific inhibition of GSK-3beta. Proc. Natl. Acad. Sci. USA *105*, 20746–20751.

Hogenesch, J.B., and Ueda, H.R. (2011). Understanding systems-level properties: timely stories from the study of clocks. Nat. Rev. Genet. *12*, 407–416.

Huang, C.Y., and Ferrell, J.E., Jr. (1996). Ultrasensitivity in the mitogen-activated protein kinase cascade. Proc. Natl. Acad. Sci. USA *93*, 10078–10083.

Isojima, Y., Nakajima, M., Ukai, H., Fujishima, H., Yamada, R.G., Masumoto, K.H., Kiuchi, R., Ishida, M., Ukai-Tadenuma, M., Minami, Y., et al. (2009). CKIepsilon/δ-dependent phosphorylation is a temperature-insensitive, period-determining process in the mammalian circadian clock. Proc. Natl. Acad. Sci. USA *106*, 15744–15749.

Johnson, C.H., Mori, T., and Xu, Y. (2008). A cyanobacterial circadian clockwork. Curr. Biol. *18*, R816–R825.

Kholodenko, B.N. (2000). Negative feedback and ultrasensitivity can bring about oscillations in the mitogen-activated protein kinase cascades. Eur. J. Biochem. *267*, 1583–1588.

Kholodenko, B.N. (2006). Cell-signalling dynamics in time and space. Nat. Rev. Mol. Cell Biol. *7*, 165–176.

Kume, K., Zylka, M.J., Sriram, S., Shearman, L.P., Weaver, D.R., Jin, X., Maywood, E.S., Hastings, M.H., and Reppert, S.M. (1999). mCRY1 and mCRY2 are essential components of the negative limb of the circadian clock feedback loop. Cell *98*, 193–205.

Lee, C., Etchegaray, J.P., Cagampang, F.R., Loudon, A.S., and Reppert, S.M. (2001). Posttranslational mechanisms regulate the mammalian circadian clock. Cell *107*, 855–867.

Lee, C., Weaver, D.R., and Reppert, S.M. (2004). Direct association between mouse PERIOD and CKIepsilon is critical for a functioning circadian clock. Mol. Cell. Biol. *24*, 584–594.

Lee, H.M., Chen, R., Kim, H., Etchegaray, J.P., Weaver, D.R., and Lee, C. (2011). The period of the circadian oscillator is primarily determined by the balance between casein kinase 1 and protein phosphatase 1. Proc. Natl. Acad. Sci. USA *108*, 16451–16456.

Legewie, S., Blüthgen, N., and Herzel, H. (2006). Mathematical modeling identifies inhibitors of apoptosis as mediators of positive feedback and bistability. PLoS Comput. Biol. *2*, e120.

Legewie, S., Schoeberl, B., Blüthgen, N., and Herzel, H. (2007). Competing docking interactions can bring about bistability in the MAPK cascade. Biophys. J. *93*, 2279–2288.

Liu, P., Kevrekidis, I.G., and Shvartsman, S.Y. (2011). Substrate-dependent control of ERK phosphorylation can lead to oscillations. Biophys. J. *101*, 2572–2581.

Lowrey, P.L., Shimomura, K., Antoch, M.P., Yamazaki, S., Zemenides, P.D., Ralph, M.R., Menaker, M., and Takahashi, J.S. (2000). Positional syntenic cloning and functional characterization of the mammalian circadian mutation tau. Science *288*, 483–492.

Maier, B., Wendt, S., Vanselow, J.T., Wallach, T., Reischl, S., Oehmke, S., Schlosser, A., and Kramer, A. (2009). A large-scale functional RNAi screen reveals a role for CK2 in the mammalian circadian clock. Genes Dev. *23*, 708–718.

Markevich, N.I., Hoek, J.B., and Kholodenko, B.N. (2004). Signaling switches and bistability arising from multisite phosphorylation in protein kinase cascades. J. Cell Biol. *164*, 353–359.

Meng, Q.J., Logunova, L., Maywood, E.S., Gallego, M., Lebiecki, J., Brown, T.M., Sládek, M., Semikhodskii, A.S., Glossop, N.R., Piggins, H.D., et al. (2008). Setting clock speed in mammals: the CK1 epsilon tau mutation in mice accelerates circadian pacemakers by selectively destabilizing PERIOD proteins. Neuron *58*, 78–88.

Meng, Q.J., Maywood, E.S., Bechtold, D.A., Lu, W.Q., Li, J., Gibbs, J.E., Dupré, S.M., Chesham, J.E., Rajamohan, F., Knafels, J., et al. (2010). Entrainment of disrupted circadian behavior through inhibition of casein kinase 1 (CK1) enzymes. Proc. Natl. Acad. Sci. USA *107*, 15240–15245.

Nakajima, M., Imai, K., Ito, H., Nishiwaki, T., Murayama, Y., Iwasaki, H., Oyama, T., and Kondo, T. (2005). Reconstitution of circadian oscillation of cyanobacterial KaiC phosphorylation in vitro. Science *308*, 414–415.

Nishiwaki, T., Satomi, Y., Kitayama, Y., Terauchi, K., Kiyohara, R., Takao, T., and Kondo, T. (2007). A sequential program of dual phosphorylation of KaiC as a basis for circadian rhythm in cyanobacteria. EMBO J. *26*, 4029–4037.

Novák, B., and Tyson, J.J. (2008). Design principles of biochemical oscillators. Nat. Rev. Mol. Cell Biol. *9*, 981–991.

O'Neill, J.S., and Reddy, A.B. (2011). Circadian clocks in human red blood cells. Nature *469*, 498–503.

Okamura, H., Miyake, S., Sumi, Y., Yamaguchi, S., Yasui, A., Muijtjens, M., Hoeijmakers, J.H., and van der Horst, G.T. (1999). Photic induction of mPer1 and mPer2 in cry-deficient mice lacking a biological clock. Science *286*, 2531–2534.

Partch, C.L., Shields, K.F., Thompson, C.L., Selby, C.P., and Sancar, A. (2006). Posttranslational regulation of the mammalian circadian clock by cryptochrome and protein phosphatase 5. Proc. Natl. Acad. Sci. USA *103*, 10467–10472.

Pittendrigh, C.S. (1954). On temperature independence in the clock system controlling emergence time in *Drosophila*. Proc. Natl. Acad. Sci. USA *40*, 1018–1029.

Plimpton, S., Battaile, C., Chandross, M., Holm, L., Thompson, A., Tikare, V., Wagner, G., Webb, E., Zhou, X., Garcia-Cardona, C., et al. (2009). Crossing the

mesoscale no-man's land via parallel kinetic Monte Carlo. Sandia Report SAND2009-6226.

Qiao, L., Nachbar, R.B., Kevrekidis, I.G., and Shvartsman, S.Y. (2007). Bistability and oscillations in the Huang-Ferrell model of MAPK signaling. PLoS Comput. Biol. *3*, 1819–1826.

Reppert, S.M., and Weaver, D.R. (2002). Coordination of circadian timing in mammals. Nature *418*, 935–941.

Rust, M.J., Markson, J.S., Lane, W.S., Fisher, D.S., and O'Shea, E.K. (2007). Ordered phosphorylation governs oscillation of a three-protein circadian clock. Science *318*, 809–812.

Sato, T.K., Yamada, R.G., Ukai, H., Baggs, J.E., Miraglia, L.J., Kobayashi, T.J., Welsh, D.K., Kay, S.A., Ueda, H.R., and Hogenesch, J.B. (2006). Feedback repression is required for mammalian circadian clock function. Nat. Genet. *38*, 312–319.

Schlosser, A., Vanselow, J.T., and Kramer, A. (2005). Mapping of phosphorylation sites by a multi-protease approach with specific phosphopeptide enrichment and NanoLC-MS/MS analysis. Anal. Chem. *77*, 5243–5250.

Schmutz, I., Wendt, S., Schnell, A., Kramer, A., Mansuy, I.M., and Albrecht, U. (2011). Protein phosphatase 1 (PP1) is a post-translational regulator of the mammalian circadian clock. PLoS ONE *6*, e21325.

Shankaran, H., Ippolito, D.L., Chrisler, W.B., Resat, H., Bollinger, N., Opresko, L.K., and Wiley, H.S. (2009). Rapid and sustained nuclear-cytoplasmic ERK oscillations induced by epidermal growth factor. Mol. Syst. Biol. *5*, 332.

Strogatz, S.H. (1994). Nonlinear Dynamics and Chaos: With Applications to Physics, Biology, Chemistry, and Engineering (Reading, MA: Addison-Wesley).

Takahashi, J.S., Hong, H.K., Ko, C.H., and McDearmon, E.L. (2008). The genetics of mammalian circadian order and disorder: implications for physiology and disease. Nat. Rev. Genet. *9*, 764–775.

Takano, A., Shimizu, K., Kani, S., Buijs, R.M., Okada, M., and Nagai, K. (2000). Cloning and characterization of rat casein kinase 1epsilon. FEBS Lett. *477*, 106–112.

Thomson, M., and Gunawardena, J. (2009). Unlimited multistability in multisite phosphorylation systems. Nature *460*, 274–277.

Toh, K.L., Jones, C.R., He, Y., Eide, E.J., Hinz, W.A., Virshup, D.M., Ptácek, L.J., and Fu, Y.H. (2001). An hPer2 phosphorylation site mutation in familial advanced sleep phase syndrome. Science *291*, 1040–1043.

Tsuchiya, Y., Akashi, M., Matsuda, M., Goto, K., Miyata, Y., Node, K., and Nishida, E. (2009). Involvement of the protein kinase CK2 in the regulation of mammalian circadian rhythms. Sci. Signal. *2*, ra26.

Ueda, H.R., Hayashi, S., Chen, W., Sano, M., Machida, M., Shigeyoshi, Y., Iino, M., and Hashimoto, S. (2005). System-level identification of transcriptional circuits underlying mammalian circadian clocks. Nat. Genet. *37*, 187–192.

Ukai-Tadenuma, M., Yamada, R.G., Xu, H., Ripperger, J.A., Liu, A.C., and Ueda, H.R. (2011). Delay in feedback repression by cryptochrome 1 is required for circadian clock function. Cell *144*, 268–281.

van Zon, J.S., Lubensky, D.K., Altena, P.R., and ten Wolde, P.R. (2007). An allosteric model of circadian KaiC phosphorylation. Proc. Natl. Acad. Sci. USA *104*, 7420–7425.

Vanselow, K., Vanselow, J.T., Westermark, P.O., Reischl, S., Maier, B., Korte, T., Herrmann, A., Herzel, H., Schlosser, A., and Kramer, A. (2006). Differential effects of PER2 phosphorylation: molecular basis for the human familial advanced sleep phase syndrome (FASPS). Genes Dev. *20*, 2660–2672.

Vielhaber, E., Eide, E., Rivers, A., Gao, Z.H., and Virshup, D.M. (2000). Nuclear entry of the circadian regulator mPER1 is controlled by mammalian casein kinase I epsilon. Mol. Cell. Biol. *20*, 4888–4899.

von Gall, C., Noton, E., Lee, C., and Weaver, D.R. (2003). Light does not degrade the constitutively expressed BMAL1 protein in the mouse suprachiasmatic nucleus. Eur. J. Neurosci. *18*, 125–133.

Walton, K.M., Fisher, K., Rubitski, D., Marconi, M., Meng, Q.J., Sládek, M., Adams, J., Bass, M., Chandrasekaran, R., Butler, T., et al. (2009). Selective inhibition of casein kinase 1 epsilon minimally alters circadian clock period. J. Pharmacol. Exp. Ther. *330*, 430–439.

Xu, Y., Padiath, Q.S., Shapiro, R.E., Jones, C.R., Wu, S.C., Saigoh, N., Saigoh, K., Ptácek, L.J., and Fu, Y.H. (2005). Functional consequences of a CKIdelta mutation causing familial advanced sleep phase syndrome. Nature *434*, 640–644.

Xu, Y., Toh, K.L., Jones, C.R., Shin, J.Y., Fu, Y.H., and Ptácek, L.J. (2007). Modeling of a human circadian mutation yields insights into clock regulation by PER2. Cell *128*, 59–70.

Young, M.W., and Kay, S.A. (2001). Time zones: a comparative genetics of circadian clocks. Nat. Rev. Genet. *2*, 702–715.